Calorimetric study of the early stages of the nanosilica - tricalcium silicate hydration. Effect of temperature

I.F. Sáez del Bosque[a], S. Martínez-Ramírez[a,b], M.T. Blanco-Varela[a]✉

a. Instituto de Ciencias de la Construcción Eduardo Torroja (IETcc-CSIC), (Madrid, Spain)
b. Instituto de Estructura de la Materia (IEM-CSIC), (Madrid, Spain)
✉ blancomt@ietcc.csic.es

ABSTRACT: The pozzolanic reaction of nanosilica in contact with C_3S was monitored via isothermal conduction calorimetry. Since that reaction is affected by heat, its variations with curing temperature (25, 40 and 65 °C) were also analysed. The findings showed that while C_3S hydration was accelerated by both nSA and higher curing temperature, the former impacted the reaction more intensely. Moreover, the presence of nSA was observed to shorten the acceleration stage during C_3S hydration, inducing earlier precipitation of portlandite and earlier C-S-H precipitation and nucleation.

KEYWORDS: Calorimetry; Tricalcium silicate; Hydration; Temperature; Nanosilica

RESUMEN: *Estudio calorimétrico de las etapas iniciales de la hidratación del silicato tricálcio- nanosílice. Efecto de la temperatura*. El estudio de la reacción puzolánica de la nanosilice en contacto con C_3S se siguió por calorimetría de conducción isotérmica. Puesto que la temperatura modifica dicha reacción, también se analizó dicho efecto (25 °C, 40 °C y 65 °C). Los resultados obtenidos mostraron que la adición de nSA al C_3S acelera su hidratación, del mismo modo que cuando se aplica temperatura de curado. Sin embargo, la adición de nSA acelera la hidratación del C_3S en mayor medida que la temperatura de curado. Además, la adición de nSA conduce a una reducción del periodo de aceleración durante la hidratación del C_3S y por tanto conduce a una temprana precipitación de portlandita y también a una temprana precipitación y nucleación de gel C-S-H.

PALABRAS CLAVE: Calorimetría; Silicato tricálcico; Hidratación; Temperatura; Nanosílice

1. INTRODUCTION

The environmental problems stemming from the CO_2 emissions generated during cement manufacture have driven studies on new additions to reduce the proportion of clinker in cement and with it the amount of CO_2 released into the atmosphere (1, 2). In recent years a good deal of interest has arisen around the application of new materials, especially nanomaterials, as additions. One of the foremost such substances is nanosilica, which in addition to acting as a nano-filler and nucleation site for C-S-H gel formation (3) (intrinsic features of nanomaterials), is a pozzolan that reduces the amount of portlandite generated in silicate hydration and furthers the C-S-H gel formation, thereby enhancing the strength, reducing the porosity and favouring the durability of the end product.

As an amorphous material with high reactive silica content, nSA, when in contact with the portlandite generated during tricalcium silicate hydration, forms additional C-S-H gel, i.e., other than the gel produced during cement hydration (pozzolanic reaction). The presence of nSA as an addition in cement pastes has been shown to modify the microstructure of the C-S-H gel formed, which has a longer mean chain length than the gels resulting from silicate hydration only (4). The presence of nanosilica and the formation of additional C-S-H gel have also been shown to be able to lower total cement porosity and refine its pore structure, improving its mechanical properties (5) and reducing the permeability of cementitious matrices (6).

Prior studies have confirmed that nSA particles serve as nucleation sites for seeding C-S-H gel, further accelerating alite hydration (7). Such acceleration raises the total heat released during silicate hydration in cements (7). Inasmuch as the pozzolanic reaction is modified by temperature (8), essentially during the early phase of hydration, the present conduction calorimetric study aimed to determine the effect of temperature on the pozzolanic reaction of nSA, in $C_3S+10\%$ nSA pastes.

2. EXPERIMENTAL

Prior characterisation of the nSA used showed its particles to be very small (20–30 nm), its N_2 BET-determined specific surface to be high (371 ± 2 m^2/g) and its content to consist primarily of amorphous SiO_2 (~90%) (4). The tricalcium silicate (C_3S) used was laboratory synthesised by firing calcium carbonate with silica gel. The XRD, ^{29}Si MAS NMR and DTA findings showed that it was a triclinic T_I polymorph with an N_2-BET-determined specific surface of 0.4 m^2/g (4).

Blends were prepared with 90 wt% C_3S and 10 wt% nSA and 100 wt% C_3S was used as the control.

Calorimetric readings were taken at three curing temperatures (25, 40 and 65 °C) with a Thermometric TAM Air analyser fitted with eight calorimetric channels having twin chambers, with each channel able to operate separately. The sample was placed in one of the chambers and water (used as a reference in accordance with the literature (9, 10)) in sufficient amounts to have the same heat capacity as the paste studied in the other. The pastes (C_3S or C_3S+nSA) were mixed with a spatula for 3 minutes outside the calorimeter in ampoules, which were then placed immediately into the chambers where measurements were recorded over a total of 72 hours. The samples containing nSA were dry blended prior to preparing the pastes.

The water/solid ratio (w/s) used to hydrate the 100 wt% C_3S was 0.425, whereas the ratio for the 90 wt% C_3S+10 wt% nSA blend was raised to 0.7 to accommodate the addition's greater water demand.

The use of admixtures to reduce the amount of water in the nSA-containing pastes was ruled out because they modify hydration kinetics. In this study it was deemed more suitable to use pastes with similar workability and consistency.

The calorimetric curves shown hereunder refer not to the total paste, but are normalised per gram of solid (C_3S or C_3S+nSA).

Acetone was added to both pastes (100 wt% C_3S and 90 wt% C_3S+10 wt% nSA) at 25, 40 and 65 °C after each heat flow peak and at the age of 24 hours to detain hydration. The pastes were then studied by differential thermal analysis and thermogravimetry (DTA/TGA). The DTA/TGA analyses were conducted on a TA Instruments SATQ600 thermal analyzer (TA instruments, New Castle, DE) in a dynamic nitrogen atmosphere in which the samples were heated at a rate of 4 °C/min from the ambient temperature to 1050 °C.

Specific surface was measured on a Micrometrics ASAP 2010, using a flow of N_2-77K. The relative adsorption pressure ranged from 0.003 to 0.3.

3. RESULTS AND DISCUSSION

When monitored with isothermal conduction calorimetry (Figure 1), C_3S hydration at 25 °C, exhibited five stages: 1) pre-induction or initial dissolution; 2) induction; 3) acceleration; 4) deceleration; 5) diffusion (11).

1) Initial dissolution period

The first stage of hydration, when in the first few minutes of the reaction calcium and silica pass rapidly into solution, could not be monitored on all the calorimetric curves because the pastes were prepared outside the calorimeter. This stage was
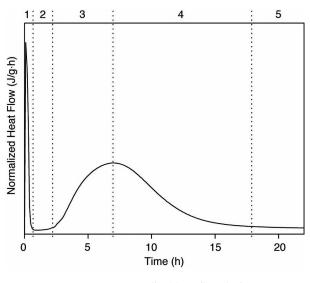

FIGURE 1. Normalised heat flow during triclinic T_I C_3S hydration at 25 °C.
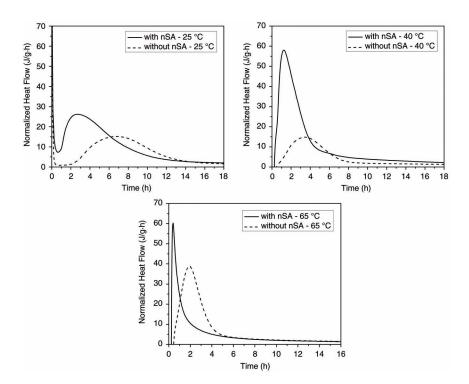
FIGURE 2.   Normalised heat flow curves for 100 wt% C_3S and 90 wt% C_3S+10 wt% nSA hydration at 25, 40 and 65 °C.

consequently observed in the 25 °C samples only and then only partially (Figure 2).

2) Induction period

In the second or induction stage (likewise only observable in pastes cured at 25 °C), the heat flow rate was lower than in the preceding stage. In general, rising temperature has also been reported to shorten the duration of this stage (11).

A number of theories (protective layer, semipermeable layer, C-S-H nucleation and growth rates, CH nucleation, crystallographic defects) have been put forward to explain the decline in heat flow during the induction stage in alite hydration (11–14). Juilland et al. (14) proposed a mechanism based on geochemical data, noting that during induction period the concentration of Ca^{2+} and OH^- ions rose, with portlandite reaching supersaturation. C-S-H gel precipitation also began in this stage and rapid hydrates growth led to supersaturation of the solution. That induced speedy consumption of the dissolved silicon ions, curbing alite dissolution and bringing the induction stage to an end.

The presence of nSA shortened this second stage, which in the pure C_3S pastes ended at 0.79 hours and in the blended pastes at 0.61 hours. Moreover, heat flow during induction was greater in the pastes containing nSA (7.32 J/g·h) than in the unblended materials (0.82 J/g·h). In the latter, the rate of heat released after the dissolution peak remained at around zero, denoting a possible pause in silicate hydration. In the blended pastes, in contrast, the heat released value was one order of magnitude higher. Both the higher heat flow and the shorter induction period suggested an increase in the rate of C_3S dissolution and stimulation of C-S-H gel nucleation and growth. The nSA-mediated pozzolanic reaction might prevent the supersaturation of Ca^{2+} and OH^- ions and stimulate the C_3S dissolution. Rapid C-S-H gel precipitation and growth would remove the Ca^{2+} ions from the medium, furthering C_3S dissolution and thereby shortening the induction stage. The high specific surface of nSA may be another factor that would shorten induction in the nSA-bearing pastes. Other authors (15) have reported shorter induction stages in C_3S hydration with the use of other nanomaterials such as nano-$CaCO_3$. Such findings run counter, however, to the Land et al. (7) observations, according to which the addition of nanosilica to white cement lengthened the induction stage slightly.

3) and 4) acceleration and deceleration periods

The following two stages of hydration (acceleration and deceleration period) constituted the main exothermal signal on all the heat flow curves for the C_3S pastes with and without nSA at the three curing temperatures shown in Figure 2.

During acceleration, the reaction rate depended on uneven C-S-H gel nucleation and growth on the tricalcium silicate and the opportunity for growth on the surface of other phases (16). The reaction rate during deceleration has been believed to be governed

by diffusion, although other factors, including the consumption of small particles (whereby only larger particles would be available to react) or the lack of space or water, may have also played a significant role (16, 17). Recent findings revealed that diffusion does not explain changes in the hydration rate between the acceleration and deceleration stages and that the impingement of different domains of the growing hydration product reduces the surface available for growth. That would readily explain the shift from the accelerating to the decelerating hydration rates (17–20), although diffusion may govern the rate in later stages of deceleration (17).

An analysis of the calorimetric curves for the nSA-free samples revealed that the exothermal peak appeared earlier and heat flow was greater at the higher curing temperatures (Table 1), confirming earlier findings to the effect that temperature accelerated the initial C_3S (4) or alite (21) hydration rate.

The steeper slope on the acceleration stage exothermal peak at higher curing temperatures was tantamount to a shorter duration. Since ex-situ preparation precluded visualising the induction stage in the 40 and 65 °C pastes, that stage may be regarded to have ended at approximately t=18 min, the time at which equilibrium was reached between the reference and the experimental sample. The duration of the acceleration stage may therefore be calculated as the difference between the time when the exothermal peak reached its maximum value and the end of the induction stage. Hence, acceleration lasted 5.03, 3.17 and 1.55° h at 25 °C, 40 °C and 65 °C, respectively. The peak was, moreover, observed to be narrower at higher temperatures, indicating a shorter deceleration stage, which in this paper was calculated as the difference between the diffusion start time (heat flow between consecutive values lower than 0.01 J/g·h) and the time when the exothermal peak reached its maximum value. The length of that stage in pastes cured at 25 °C was 10 h, compared to 5.72 and 5.01 h in the 40 and 65 °C pastes, respectively.

Despite the dilution induced by the addition of nSA (2.7 g of C_3S compared to 3 g in the pure pastes),

both total heat and the heat flow at the exothermal peak were observed to be greater than in the unblended pastes at all curing temperatures (see Table 2 and the samples cured at 25 °C, Figure 3). Some authors contend that the higher the water/solid ratio in the mix, the longer is the time of appearance of the maximum heat flow peak (21, 22). In the present study, however, the peak appeared earlier in the blended (w/s=0.7) than in the unblended (w/s=0.45) pastes. All the foregoing supports the premise that the nSA-mediated pozzolanic reaction lowered the concentration of Ca^{2+} ions in the solution according with other pozzolans (23), leading to re-dissolution of C_3S, accelerating its initial hydration and contributing to greater heat flow. At the same time, nanoparticles such as nSA may act a seed for hydration product crystallisation, thereby heightening cement hydration (24), which would in turn contribute to greater heat flow. Furthermore, the formation of additional C-S-H gel with the pozzolanic reaction could also have contributed to raising the heat flow in the blended pastes. According to a study by Alizadeh et al. (25), the addition of synthetic C-S-H gel (synthesised with stoichiometric amounts of CaO and SiO_2) accelerated C_3S hydration. That would be similar to the effect that must be caused by the pozzolanic reaction and is consistent with the results reported by Land et al. (7). These authors likewise observed a rise in heat flow when white cement hydration was doped with nanosilica and reported that the higher the specific surface of the nSA, the greater was the amount of heat released. Moreover, this initial acceleration of C_3S hydration brought C-S-H gel formation and portlandite precipitation forward.

Figure 4 shows the rate of heat released per gram of tricalcium silicate: note that in the absence of nanosilica, temperatures of 65 °C were needed to generate any material rise in heat flow. In the presence of nSA, however, such a rise was attained at a
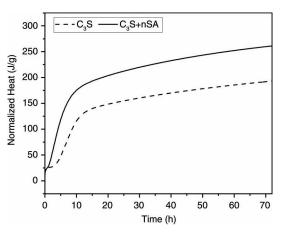
TABLE 1. Isothermal conduction calorimetry data for C_3S hydrated at 25 °C, 40 °C and 65 °C

	25 °C	40 °C	65 °C
Maximum normalised heat flow (J/g·h)	15.17	14.85	38.80
Time (h)	6.84	3.47	1.85

TABLE 2. Isothermal conduction calorimetry results for 90 wt% C_3S+10 wt% nSA hydration at 25 °C, 40 °C and 65 °C

	25 °C	40 °C	65 °C
Maximum normalised heat Flow (J/g·h)	26.2	58.1	60.32
Time (h)	2.72	1.23	0.40

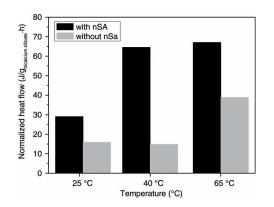FIGURE 3. Normalised heat of C_3S hydration in 100 wt% C_3S and 90 wt% C_3S+10 wt% nSA at 25 °C.

FIGURE 4. Normalised heat flow per gram of C$_3$S during hydration of 100 wt% C$_3$S and 90 wt% C$_3$S+10 wt% nSA at 25, 40 and 65 °C (values for maximum heat flow).

also its width, which narrowed at higher curing temperatures due to the shorter duration of the acceleration stage (1.73, 0.97 and 0.1 h at 25 °C, 40 °C and 65 °C, respectively). That shorter duration denoted acceleration of C$_3$S hydration in the presence of nSA due to the pozzolanic reaction, which consumed the portlandite generated during silicate hydration and produced additional C-S-H gel. Further to Thomas et al. (3), the additional C-S-H gel thus formed would seed the formation of more gel from the silicates. However, the length of deceleration stage was compared to the nSA-free pastes, (13.50, 9.27 and 5.48 h at 25, 40 and 65 °C, respectively).

The calorimetric curves for the pastes studied suggested that nSA pozzolanicity was intense enough to react with portlandite during the acceleration period as well as to hasten C$_3$S hydration. The pastes were hydrated at three test temperatures to verify these two effects. Hydration was detained both at the end of the acceleration period and when the flow of heat released peaked. The pastes obtained were analysed with TG (Figure 5) and FTIR (Figure 6).

The three nSA-free pastes lost mass at 25 to ≈390 °C due to the evaporation of chemically combined water in the C-S-H gel forming. A second phase of mass loss was observed in the 398–453 °C range, characteristic of the thermal dehydroxylation of portlandite. The rise in intensity of this loss with
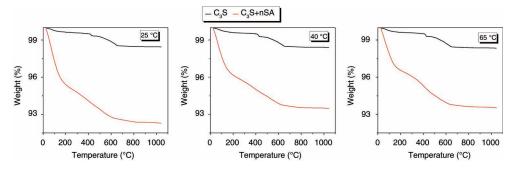
lower curing temperature, 40 °C. Even at 25 °C, the addition of nanosilica raised heat flow significantly, while the 65 °C pastes containing nSA released nearly double the heat recorded for the unblended pastes. Both nanosilica and temperature raised the heat flow rate in initial C$_3$S hydration, although the effect of the addition was more intense.

As in the nSA-free pastes, changes were observed in the exothermal peak on the calorimetric curve for the blended pastes, affecting not only in its slope but

FIGURE 5. TG analysis of 100 wt% C$_3$S and 90 wt% C$_3$S+10 wt% nSA at 25, 40 y 65 °C (values for maximum heat flow).
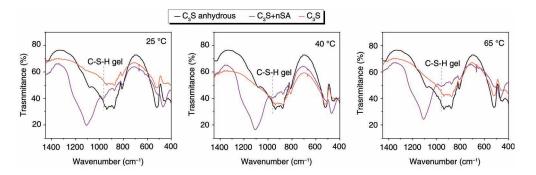

FIGURE 6. FTIR spectra of anhydrous C$_3$S and hydrated 100 wt% C$_3$S and 90 wt% C$_3$S+10 wt% nSA pastes at 25, 40 and 65 °C (values for maximum heat flow).
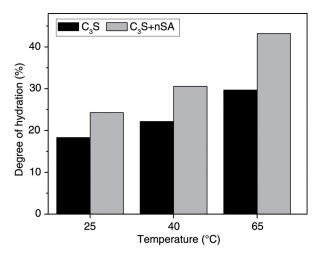
FIGURE 7.   Degree of hydration of 100 wt% C_3S and 90 wt% C_3S+10 wt% nSA at 25, 40 and 65 °C over 24 h.

curing temperature was attributable to the accelerating effect of temperature on C_3S hydration. All three samples exhibited mass loss at 453 to 673 °C. Interpreted as a loss of CO_2, this was an indication that they were carbonated during handling. The scant total loss recorded (1.5–1.66%) speaks to the low degree of reaction attained at the test times.

None of the nSA-containing samples exhibited signs of portlandite dehydroxylation, confirming that nSA reacted with portlandite in the acceleration period of C_3S hydration even in the samples hydrated at 25 °C. The total mass loss was much greater in these samples (6.5–7.52 %) than in the pure C_3S pastes, a sign that the C_3S-water reaction had progressed much farther due to the presence of nSA, despite the shorter times at which hydration was detained.

The FTIR spectra also confirmed that nSA accelerated C_3S hydration. All the spectra for the nSA samples contained a C-S-H gel band at around 965 cm^{-1}, attributed, further to Yu et al. (26), to

Q^2 units. In the spectra for the samples without the addition the band was much less intense and overlapped with the bands for anhydrous C_3S. Furthermore, in the nSA-additioned samples, the intensity of the bands characteristic of anhydrous C_3S declined with rising curing temperature, denoting greater C_3S hydration due to the effect of temperature.

5) diffusion period

After 24h, hydration was governed by diffusion in pastes both with and without nSA, which exhibited similar heat flow rates, ranging from 1 to 1.5 J/g·h. The ^{29}Si MAS NMR findings on degree of hydration showed that more C-S-H gel formed and the degree of C_3S hydration was greater both at higher temperatures and in the presence of nSA (Figure 7) (4). Furthermore, at that age, TG studies revealed differences in the total portlandite (CH+$CaCO_3$) present in the samples. The amount of portlandite, after 24 hours of hydration, rose slightly with higher curing temperatures in the unblended pastes (Figure 8a). In the pastes containing nSA, however, the amount of portlandite rose substantially at 25 °C as a result of the higher degree of hydration induced in the C_3S. That effect declined with temperature as a result of the higher intensity of the pozzolanic reaction in the blended pastes. Moreover, in the 24 h nSA-bearing samples, the amount of water bound to the C-S-H gel (defined as the total mass loss at 1 000 °C less the loss attributed to portlandite dehydroxylation and carbonate decarbonation, Figure 8b) rose substantially, attesting to a speedier water-C_3S reaction due to the presence of nSA. In other words, the amount of C-S-H gel was greater in the nSA samples, a finding wholly consistent with the higher degrees of hydration detected with ^{29}Si MAS-NMR.

4. CONCLUSIONS

The conclusions that may be drawn around the effect of curing temperature and the addition of nSA on C_3S hydration are listed below.
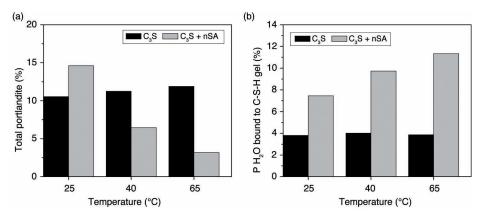

FIGURE 8.   (a) Total portlandite and (b) H_2O bound to C-S-H generated in 24 hours of hydration of 100 wt% C_3S and 90 wt% C_3S+10 wt% nSA at 25, 40 and 65 °C.

The addition of nSA accelerates C_3S hydration regardless of curing temperature, raising the amount of heat released during hydration. Of course, curing temperature accelerates C_3S hydration, generating greater heat flow rates at earlier times, but the accelerating effect of nSA is more intense than the effect of curing temperature, within the limits proposed in the present study.

Adding nSA induces early portlandite precipitation and early C-S-H gel precipitation and nucleation at 25 °C. These factors together with nSA high specific surface reduce induction period.

The addition of nSA also shortens the acceleration stage and lengthen the deceleration stage of C_3S hydration at 25 °C, 40 °C and 65 °C.

ACKNOWLEDGEMENTS

REFERENCES

1. Lin, L-K.; Wu, W-S.; Lee, H. (2013). Value analysis and properties investigation of high performance rice husk ash concrete. *Adv. Mat. Res*. http://dx.doi.org/10.4028/www.scientific.net/AMR.773.293.
2. Fairbairn, E.M.R.; Americano, B.B.; Cordeiro, G.C.; Paula, T.P.; Toledo Filho, R.D.; Silvoso, M.M. (2010). Cement replacement by sugar cane bagasse ash: CO_2 emissions reduction and potential for carbon credits. *J. Environ. Manag*. 91, 1864–1871. http://dx.doi.org/10.1016/j.jenvman.2010.04.008.
3. Thomas, J.J.; Jennings, H.M.; Chen, J.J. (2009) Influence of Nucleation Seeding on the Hydration Mechanisms of Tricalcium Silicate and Cement. *J. Phys. Chem. C* 113, 4327–4334. http://dx.doi.org/10.1021/jp809811w.
4. Sáez del Bosque, I.F.; Martín-Pastor, M.; Martínez-Ramírez, S.; Blanco-Varela, M.T. (2013) Effect of temperature on C_3S and C_3S+ nanosilica hydration and C-S-H gel structure. *J. Am. Ceram. Soc*. 96, 957–965. http://dx.doi.org/10.1111/jace.12093.
5. Kontoleontos, F.; Tsakiridis, P.E.; Marinos, A.; Kaoidas, V.; Katsioti, M. (2012) Influence of colloidal nanosilica on ultrafine cement hydration: Physicolchemical and microstructural characterization. *Constr. Build. Mater*. 35, 347–360. http://dx.doi.org/10.1016/j.conbuildmat.2012.04.022.
6. Ozyildirim, C.; Zegetosky, C. (2010) Exploratory investigation of nanomaterials to improve strength and permeability of concrete. *Transport. Res*. 2142, 1–2148.
7. Land, G.; Stephan, D. (2012) The influence of nano-silica on the hydration of ordinary Portland cement. *J. Mater. Scienc*. 47, 1011–1017. http://dx.doi.org/10.1007/s10853-011-5881-1.
8. Tashima, M.M.; Soriano, L.; Monzó, J.; Borrachero, M.V.; Akasaki, J.L.; Payá, J. (2014) New method to assess the pozzolanic reactivity of mineral admixtures by means of pH and electrical conductivity measurements in lime:pozzolan suspensions. *Mater. Construcc*. 64, e032. http://dx.doi.org/10.3989/mc.2014.00914.
9. Wadsö, L. (2010) Operational issues in isothermal calorimetry. *Cem. Concr. Res*. 40, 1129–1137. http://dx.doi.org/10.1016/j.cemconres.2010.03.017.
10. Quennoz, A. (2011) Hydration of C_3A with Calcium Sulfate Alone and in the Presence of Calcium Silicate. *Thesis doctoral. EPFL*.
11. Barnes, P. (1983). *Structure and Performance of Cement*. Applied Science Publishers, London, UK.
12. Taylor, H.F.W. (1997) *Cement Chemistry*. Academia Press, London, U.K.
13. Makar, J.M.; Chan, G.W. (2008) End of the induction period in ordinary portland cement as examined by high-resolution scanning electron microscopy. *J. Am. Ceram. Soc*. 91, 1292–1299.
14. Juilland, P.; Gallucci, E.; Flatt, R.; Scrivener, K. (2010) Dissolution theory applied to the induction period in alite hydration. *Cem. Concr. Res*. 40, 831–844. http://dx.doi.org/10.1016/j.cemconres.2010.01.012.
15. Sato, M.; Diallo, F. (2010) Seeding Effect of Nano-$CaCO_3$ on the hydration of Tricalcium Silicate. *Transportation Research Record* 2141, 61–67. http://dx.doi.org/10.3141/2141-11.
16. Noor-ul-Amin; Alam, S.; Gaul, S.; Muhammad, K. (2013) Hydration mechanism of tricalcium silicate (alite). *Adv. Cem. Res*. 25, 60–68. http://dx.doi.org/10.1680/adcr.11.00061.
17. Bullard, J.W.; Jennings, H.M.; Livingston, R.A.; Nonat, A.; Scherer, G.W.; Schweitzer, J.S.; Scrivener, K.L.; Thomash, J.J. (2011) Mechanisms of cement hydration. *Cem. Concr. Res*. 41, 1208–1223. http://dx.doi.org/10.1016/j.cemconres.2010.09.011.
18. Thomas, J.J.; Biernacki, J.J.; Bullard, J.W.; Bishnoi, S.; Dolado, J.S.; Scherer, G.W.; Luttge, A. (2011) Modeling and simulation of cement hydration kinetics and microstructure development. *Cem. Concr. Res*. 41, 1257–1278. http://dx.doi.org/10.1016/j.cemconres.2010.10.004.
19. Thomas, J.J. (2007) A New Approach to Modeling the Nucleation and Growth Kinetics of Tricalcium Silicate Hydration. *J. Am. Ceram. Soc*. 90, 3282–3288. http://dx.doi.org/10.1111/j.1551-2916.2007.01858.x.
20. Bishnoi, S.; Scrivener, K.L. (2009) μic: A new platform for modelling the hydration of cements. *Cem. Concr. Res*. 39, 266–274. http://dx.doi.org/10.1016/j.cemconres.2008.12.002.
21. Zákoutský, J.; Tydlitát, V.; Cerný, R. (2012) Effect of temperature on the early-stage hydration characteristics of Portland cement: A large-volume calorimetric study. *Constr. Build. Mater*. 36, 969–976. http://dx.doi.org/10.1016/j.conbuildmat.2012.06.025.
22. Sáez del Bosque, I.F.; Martínez-Ramírez, S.; Blanco-Varela, M.T. (2012) From 30 May to 1 June. Influencia de la relación agua/sólido en la hidratación del silicato tricálcico y de dos cementos portland comerciales (Influence of the water/solid ratio on C_3S hydration and two portland cement). In *XII Congreso Nacional de Materiales - IBEROMAT XII*. Alicante, Spain.
23. Hewlett, P.C. (1988). *Lea's Chemistry of Cement and Concrete*. Elsevier, Oxford, U.K.
24. Nazari, A.; Riahi, S. (2011) The effects of Cr_2O_3 nanoparticles on strength assessments and water permeability of concrete in different curing media. *Mater. Sci. Eng. A* 528, 1173–1182. http://dx.doi.org/10.1016/j.msea.2010.09.099.
25. Alizadeh, R.; Raki, L.; Makar, J.M.; Beaudoin, J.J.; Moudrakovski, I. (2009) Hydration of tricalcium silicate in the presence of synthetic calcium-silicate-hydrate. *J. Mater. Chem*. 19, 7937–7946. http://dx.doi.org/10.1039/B910216G.
26. Yu, P.; Kirkpatrick, R.J.; Poe, B.; McMillan, P.F.; Cong, X. (1999) Structure of calcium silicate hydrate (C-S-H): Near-, Mid-, and Far-Infrared Spectroscopy. *J. Am. Ceram. Soc*. 82, 742–748. http://dx.doi.org/10.1111/j.1151-2916.1999.tb01826.x.